Quantum Mechanical Wave Packet and Quasiclassical Trajectory Calculations for the Li + H_2^+ Reaction†

N. Bulut,‡,§ J. F. Castillo,‡ L. Bañares,*,‡ and F. J. Aoiz‡

Departamento de Química Física I, Facultad de Ciencias Químicas, Universidad Complutense de Madrid, 28040 Madrid, Spain, and Department of Physics, Firat University, 23169 Elazig, Turkey

Received: May 12, 2009; Revised Manuscript Received: June 18, 2009

The dynamics and kinetics of the Li + H_2^+ reaction have been studied by means of quantum mechanical (QM) real wave packet, wave packet with flux operator, and quasiclassical trajectory (QCT) calculations on the ab initio potential energy surface of Martinazzo et al. [*J. Chem. Phys.*, **2003**, *119*, 21]. Total initial state-selected reaction probabilities for the title reaction have been calculated for total angular momentum $J = 0$ at collision energies from threshold up to 1 eV. Wave packet reaction probabilities at selected values of the total angular momentum up to $J = 60$ are obtained using the centrifugal sudden approximation (CSA). Integral cross sections and rate constants have been calculated from the wave packet reactions probabilities by means of a refined *J*-shifting method and the separable rotation approximation in combination with the CSA for $J > 0$. The calculated rate constants as function of temperature show an Arrhenius type behavior. The QM results are found to be in overall good agreement with the corresponding QCT data.

I. Introduction

The interaction between Li atoms and ionic H_2^+ molecules is considered to be of some importance in establishing the kinetic details of the lithium chemistry during the evolution of the early universe.[1−8] Lithium chemistry in such a rarefied, dust-free environment is much more complicated than the H, D, and He counterparts because the low ionization potential of the Li species allows an effective competition between ionic and neutral processes.[5] Lithium chemistry began with radiative association reactions in which LiH and LiH^+ species were formed. Once formed, LiH is depleted by reaction with atomic hydrogen and may undergo rotational and vibrational excitation-relaxation by collisions with H and He. However, it has been found that LiH at relatively low redshifts is mainly ionized. Therefore, a correct modeling of the Li chemistry requires to consider also ionic processes.

Despite the low number of electrons the LiH_2^+ system shows all the complex features of the more complicated chemical species as it has been shown in a series of ab initio studies.[8−13] Recently global three-dimensional adiabatic potential energy surfaces (PES) for the ground and first excited states of LiH_2^+ system have been calculated and fitted by Martinazzo et al.[13] The potential energy surfaces are based on more than 11 000 ab initio points computed using a multireference valence bond approach[12] and extended with 600 points calculated by multi-reference configuration interaction (MRCI) based on complete active space self-consistent-field (CASSCF) reference functions and a large basis set. The first excited-state PES is relevant for the hydrogen-charged species reactions such as

$$\mathrm{Li} + \mathrm{H_2^+} \rightarrow \mathrm{H^+} + \mathrm{LiH} \qquad (1)$$

and its reverse

$$\mathrm{H^+} + \mathrm{LiH} \rightarrow \mathrm{H_2^+} + \mathrm{Li} \qquad (2)$$

This first excited-state PES for the Li + H_2^+ reaction, schematically shown in Figure 1, is characterized by a charge-induced dipole well 0.586 eV below the Li + H_2^+ asymptote, a deep well due to dipole-charge interaction, which lies 1.315 eV below the LiH + H^+ asymptote, and a saddle point between them which lies 0.046 eV above the Li + H_2^+ asymptote. Reaction (1) is endothermic by 0.217 eV when the zero point energies (ZPE) of the reactants and products are considered.

Dynamical calculations for the LiH_2^+ system on the first excited-state PES are scarce. In particular, Gogtas performed time dependent real wave packet (RWP) quantum dynamical calculations[14] for reaction (1) on the first excited state LiH_2^+ PES of Martinazzo et al.[13] In that work, reaction probabilities for $J = 0$ and initial state selected H_2^+ ($v = 0$, $j = 0-3$) were calculated as a function of total energy and then used to get approximate integral cross sections and thermal rate constants using a standard *J*-shifting approximation. The total reaction probabilities for $J = 0$ as a function of total energy show a threshold at around 0.5 eV and increase rather smoothly from threshold up to 1.7 eV. The observed behavior of the reaction probabilities calculated in that work suggests that resonances do not play a major role for the reaction. This fact is rather surprising because the PES exhibits deep wells and quantum reactive scattering resonances are likely to play an important role in the reaction dynamics. It is important to note that although the classical barrier of reaction (1) is 0.046 eV above the reactant's asymptote, the addition of the ZPE to H_2^+ and transition state (0.102 eV) makes the reactants to lie at about the same level than the linear Li−H−H^+ saddle point. This poses doubts on the reliability of the standard, most simple *J*-shifting model when applied to the study of the title reaction. In addition, Pino et al. have recently performed quasi-classical trajectory (QCT) calculations for the title reaction on the same first excited-state PES.[15] Thermal rate constants were calculated in the tem-

† Part of the "Vincenzo Aquilanti Festschrift".
* To whom correspondence should be addressed.
‡ Universidad Complutense de Madrid.
§ Firat University.

10.1021/jp904429e © 2009 American Chemical Society
Published on Web 07/21/2009

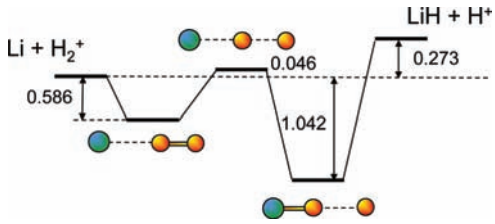

Figure 1. Schematic reaction path and energetics for the $Li + H_2^+ \rightarrow LiH + H^+$ reaction on the PES of Martinazzo et al.[13] Energies (in eV) are referred to the asymptotic valley of the $Li + H_2^+$ reactants.

perature range 600−4000 K, and found to be at variance with those reported by Gotgas.[14] Therefore, a new detailed theoretical study of the title reaction is warranted.

In a recent work, we have reported RWP and QCT[16] calculations for the reverse $H^+ + LiH$ reaction (2). State resolved and total reaction probabilities at $J = 0$ for the two possible exchange, $LiH + H^+$, and abstraction, $H_2^+ + Li$, reaction channels were presented. Integral cross sections and rate constants were also calculated. In the case of the RWP calculations, a capture model was used to estimate cross sections and rate constants. It was established that the thermal rate constants calculated by the RWP and QCT methods are nearly independent of temperature in the 100−500 K temperature range. Our results were in good agreement with those reported by Pino et al.[15] for reaction (2).

In the present work, we have extended our previous calculations to the endothermic $Li + H_2^+$ reaction (reaction (1)). RWP, wave packet with flux operator (FWP) and QCT calculations have been carried out on the first excited-state PES of Martinazzo et al.[13] Initial state-resolved reaction probabilities for $J = 0$ have been calculated and integral cross sections and rate constants have been estimated from wave packet reaction probabilities calculated for $J > 0$ using the Centrifugal Sudden approximation (CSA) in combination with refined and uniform J-shifting procedures and using the QCT method. The organization of the paper is as follows: in section II we briefly review the RWP, FWP, and QCT theoretical methods employed in this work, section III presents the main results and discussions and, finally, section IV closes with the conclusions.

II. Theory

A. Real Wave Packet Method. We have used the time-dependent RWP method developed by Gray and Balint-Kurti. The RWP method has been well documented in the literature[17−19] and only the details relevant to the present work will be given here. For the present calculations, the initial wave packet is located in the asymptotic reactant channel, where there is no influence of the interaction potential, and the propagation grid scheme is defined using the product Jacobi coordinates. The present RWP calculations are restricted to zero total angular momentum, $J = 0$. Calculations have been carried out up to 1 eV of collision energy in a fine grid in order to catch the oscillatory behavior of the reaction probabilities as a function of energy for this system. The properties of the initial wave packet and the grid parameters used for the calculations are given in Table 1.

B. Wave Packet Using the Flux Operator Method. Another time-dependent wave packet method for initial state-selected reactive scattering is based on the following expression for the reaction probabilities[20]

$$P(E) = \langle \psi(E)|F|\psi(E)\rangle \tag{3}$$

TABLE 1: Parameters Used in the RWP Calculations[a]

reactant scattering coordinate range:	$R_{min} = 0.0$; $R_{max} = 30.5$
number of grid points in R:	319
diatomic coordinate range:	$r_{min} = 0.5$; $r_{max} = 29.5$
number of grid points in r:	319
number of angular basis functions:	80
center of initial wave packet:	$R_0 = 28.5$
Gaussian width factor:	$\alpha = 0.6$
initial wave vector:	$k_0 = 7.5$
position of analysis line:	$R_\infty = 28.5$
number of Chebyshev iterations:	120 000

[a] All parameters are given in atomic units.

Here $\psi(E)$ is a reactive scattering wave function that tends asymptotically to a flux-normalized incoming wave in the reactant channel plus outgoing scattered waves in all open reactant and product channels and F is the reactive flux operator[21]

$$F = \frac{i}{\hbar}[\hat{H}, h(f(\mathbf{x}))] \tag{4}$$

where $\hat{H}$ is the Hamiltonian, $h(f(\mathbf{x}))$ is the Heaviside step function, and the equation $f(\mathbf{x}) = 0$ defines a dividing surface between reactants and products such that the reactants are in $f(\mathbf{x}) < 0$ and the products are in $f(\mathbf{x}) < 0$. The component of the scattering wave function $\psi(E)$ that crosses the dividing surface $f(\mathbf{x}) = 0$ and contributes to the reactive flux can be calculated as[22]

$$\psi(E) = \frac{1}{<\phi^+_{E\alpha v}|\chi_{\alpha v}(0)>} \int_0^\infty e^{+iEt/\hbar}\chi_{\alpha v}(t)\, dt \tag{5}$$

where

$$\chi_{\alpha v}(t) = e^{-i(H-i\varepsilon)t/\hbar}|\chi_{\alpha v}(0)| \tag{6}$$

and $\phi^+_{E\gamma v}$ is an energy normalized incoming wave in the corresponding channel. The small but finite ε term ensures the convergence of the time integral. In this work, we use the mass-scaled Jacobi coordinates R_α, r_α, and γ_α of the reactant arrangement, in terms of which the Hamiltonian $\hat{H}$ for total angular momentum $J = 0$ is[23]

$$\hat{H} = \hat{T} + \hat{U} \tag{7}$$

where

$$\hat{T} = -\frac{\hbar^2}{2\mu}\left(\frac{\partial^2}{\partial R_\alpha^{\,2}} + \frac{\partial^2}{\partial r_\alpha^{\,2}}\right) \tag{8}$$

and

$$\hat{U} = -\frac{\hbar^2}{2\mu}\left(\frac{1}{R_\alpha^{\,2}} + \frac{1}{r_\alpha^{\,2}}\right)\frac{1}{\sin\gamma_\alpha}\frac{\partial}{\partial\gamma_\alpha}\sin\gamma_\alpha\frac{\partial}{\partial\gamma_\alpha} + V(R_\alpha, r_\alpha, \gamma_\alpha) \tag{9}$$

The flux dividing surface is defined as

$$f(r_\alpha) = r_\alpha - r_{\alpha,0} \tag{10}$$

so that the reactive flux operator F becomes

$$F = -\frac{i\hbar}{2\mu}\left[\frac{\partial}{\partial r_\alpha}\delta(r_\alpha - r_{\alpha,0}) + \delta(r_\alpha - r_{\alpha,0})\frac{\partial}{\partial r_\alpha}\right] \tag{11}$$

The incoming wave $\phi^+_{E\alpha\nu}$ with $\nu = v,j$, is defined as

$$\phi^+_{E\alpha\nu} = v^{-1/2}_{E\alpha\nu} h^{(2)}_j(k_{E\alpha\nu}R_\alpha) \tag{12}$$

where $h^{(2)}_j(k_{E\alpha\nu}R_\alpha) \sim \exp[\pm i(k_{E\alpha\nu} - j\pi/2]$ is a Ricatti-Hankel function with $k_{E\alpha\nu} = (2\mu(E - E_{\alpha\nu}))^{1/2}/\hbar$ as the asymptotic wavenumber and $v = \hbar k_{E\alpha\nu}/\mu$ as the asymptotic velocity in channel $\alpha\nu$. The initial reactant wavepacket $\chi_{\alpha\nu}$ is defined as

$$\chi_{\alpha\nu} = \frac{1}{R_\alpha r_\alpha} e^{(R_\alpha - R_{0,\alpha})^2/2\delta^2 - ik_{\alpha,0}R_\alpha}\phi_\nu(r_\alpha)P_j(\cos\gamma_\alpha) \tag{13}$$

The Hamiltonian $\hat{H}$ has been represented using discrete variable representations (DVRs) for the radial coordinates R_α and r_α and a Legendre polynomial basis set is used to describe the angular coordinate γ_α. Gauss-Legendre quadrature points are employed as angular grid points. The Hamiltonian matrix in the present representation is very sparse and therefore the time evolution of the wave packet can be performed using the split operator method[24] with a partitioning of the evolution operator as

$$e^{-i\hat{H}\Delta t/\hbar} = e^{-i\hat{U}\Delta t/2\hbar}e^{-i\hat{T}\Delta t/\hbar}e^{-i\hat{U}\Delta t/2\hbar} + O(\Delta t^3) \tag{14}$$

A complex absorbing potential $V_{opt}(R_\alpha, r_\alpha)$ have been incorporated to absorb the wave packet over the last quarter of the DVR grids in R_α and r_α. The relevant parameters used in the flux wave packet (FWP) calculations are given in Table 2.

C. Approximations for $J > 0$. Reaction probabilities for $J > 0$ have been calculated using the Centrifugal Sudden Approximation (CSA), which significantly reduces the amount of computational effort[25] with respect to the exact coupled-channel (CC) calculations. The use of the CSA for a reaction mediated by resonances may not be accurate enough. However, an accurate CC calculation including the full Coriolis couplings is unpractical in the present case. The calculation of the integral cross sections as a function of collision energy for each rovibrational state v, j of the reagent molecule requires summing up all the partial wave contributions of the total angular momentum J to the reaction probabilities

$$\sigma_{v,j}(E_c) = \frac{\pi}{k^2}\frac{1}{2j+1}\sum_{J=0}(2J+1)[2\min(J,j)+1]P^J_{v,j}(E_c) \tag{15}$$

where $k = (2\mu E_c)^{1/2}/\hbar$ and $P^J_{v,j}(E_c)$ is the reaction probability from the initial rovibrational state v,j summed over all final states as a function of collision energy, E_c, at a total angular momentum J.

TABLE 2: Parameters Used in the FWP Calculations[a]

scattering coordinate range:	$R_{min} = 0.0$; $R_{max} = 30.0$
number of grid points in R:	243
diatomic coordinate range:	$r_{min} = 0.0$; $r_{max} = 30.0$
number of grid points in r:	243
number of angular basis functions:	200
center of initial wave packet:	$R_0 = 23.0$
gaussian width factor:	$\delta = 0.17$
average wave vector of initial wave packet:	$k_0 = 9.0$
truncation parameter for DVR grid:	$V_{max} = 0.06$
location of flux dividing surface:	$r_0 = 23.0$
time step for propagation:	$\Delta t = 2.0$ (0.05 fs)
propagation time:	60 000 (3 ps)

[a] All parameters are given in atomic units.

The v,j initial state-selected rate constant is calculated by averaging of the corresponding integral cross section $\sigma_{v,j}(E_c)$ over the translational energy as

$$k(T;v,j) = \left[\frac{8}{\pi\mu(k_BT)^3}\right]^{1/2}\int_0^\infty E_c\sigma_{v,j}(E_c)e^{-E_c/k_BT}\,dE_c \tag{16}$$

where k_B is the Boltzmann constant and μ is the reduced mass of the LiH_2^+ system.

In the standard J-shifting method,[26] initial v, j state-specific total reaction probabilities for $J > 0$ are calculated using

$$P^J_{v,j}(E_c) \approx P^{J=0}_{v,j}[E_c - E^J_{shift}] \tag{17}$$

where $P^{J=0}_{v,j}$ is the initial v, j quantum state-resolved reaction probability for $J = 0$ as a function of collision energy E_c, and $P^J_{v,j}(E_c)$ is the estimated reaction probability for higher values of J at energy $E_c - E^J_{shift}$, where

$$E^J_{shift} = \frac{\hbar^2}{2\mu R_0^2}J(J+1) \tag{18}$$

where R_0 is the Li−HH^+ distance at the transition state.

A more refined J-shifting approach has been applied in the present work consisting in using the specific reaction probabilities calculated within the CSA approximation at selected values of $J = 0$, 10, 20, 30, 40, 50, 60, 70, 80, and 90. Then, we calculate specific rotational constants, B^J_i, to estimate the reaction probabilities in the intervals $J \in [0, 10]$, $J \in [10, 20]$, $J \in [20, 30]$, and so on, up to $J = 90$. Thus to estimate the reaction probabilities in $J \in [J_i, J_{i+1}]$

$$P^J(E_c) \approx P^{J_i}\{E_c - B^J_i[J(J+1) - J_i(J_i+1)]\}, \quad \text{if } J_i < J < J_{i+1} \tag{19}$$

where B^J_i is evaluated using the reaction probabilities at $J = J_i$ and $J = J_{i+1}$ by equating:

$$P^{J_{i+1}}(E_c) = P^{J_i}\{E_c - B^J_i[J_{i+1}(J_{i+1}+1) - J_i(J_i+1)]\} \tag{20}$$

Substituting eq 19 in eq 15 and using eq 16, the rate constants can be directly evaluated within this approximation, assuming that a single value of B^J_i is capable of matching the reaction

probabilities at J_i and J_{i+1}. A similar approximation was originally proposed by Mielke et al.[27] and termed separable rotation approximation (SRA) (later denoted uniform J-shifting approach by Zhang and Zhang[28]). The specific rate constants are given by

$$k_{\mathrm{SRA}}(T;v,j) = \sqrt{\frac{2\pi\hbar^4}{(\mu k_{\mathrm{B}}T)^3}}Q^{J=0}(T)\sum_J \frac{2\min(J,j)+1}{2j+1} \times (2J+1)\mathrm{e}^{-B_i(T)J(J+1)/k_{\mathrm{B}}T} \quad (21)$$

where

$$Q^{J=0}(T) = \int P^{J=0}(E_{\mathrm{c}})\mathrm{e}^{-E_{\mathrm{c}}/k_{\mathrm{B}}T}\,\mathrm{d}E_{\mathrm{c}} \quad (22)$$

$$B_i(T) = \frac{k_{\mathrm{B}}T}{J_{i+1}(J_{i+1}+1) - J_i(J_i+1)}\ln\left(\frac{Q^{J_i}}{Q^{J_{i+1}}}\right) \quad (23)$$

and

$$Q^{J}(T) = \int P^{J}(E_{\mathrm{c}})\mathrm{e}^{-E_{\mathrm{c}}/k_{\mathrm{B}}T}\,\mathrm{d}E_{\mathrm{c}} \quad (24)$$

Notice that the B_i values so calculated depend on the temperature and represent an average value of the B_i^J constants evaluated using eq 20.

The method requires to calculate at least the total reaction probabilities for three values of J and can be easily generalized to cases with more than three values of J. This method is more accurate than the standard J-shifting procedure.[26]

D. Quasiclassical Trajectory Calculations. The quasiclassical trajectory method used for the calculations presented in this work has been described in detail previously (see, for instance, ref 29 and references therein) and therefore only those details relevant to the present work are given here.

Reaction probabilities as a function of collision energy for the Li + H_2^+($v = 0, j = 0$) reaction have been calculated by running a batch of $2 \cdot 10^5$ trajectories at randomly and uniformly sampled collision energies within the range 0.05−1.0 eV for zero impact parameter $b = 0$ (equivalent to $J = 0$). The calculation of total and vibrationally state-resolved reaction probabilities for $J = 0$ from the trajectory results has been performed by the method of moments expansion in Legendre polynomials and employing a Gaussian-weighted binning (GWB) procedure using 0.2 full-width-half-maximum.[30,31]

Total reaction probabilities as a function of collision energy for different values of the total angular momentum $J = 0$, 10, 20, 30, 40, 50, and 60 for the title reaction have been calculated by running batches of 2×10^5 trajectories for each value of J in the collision energy range 0.05−1.0 eV, as described in ref 29, using the expression

$$b = \frac{\hbar}{\mu v_r}[L(L+1)]^{1/2} \quad (25)$$

where b is the impact parameter of the trajectories, L is the orbital angular momentum quantum number ($L = J$ when $j = 0$) and μ and v_r are the Li−H_2^+ reduced mass and relative velocity, respectively. The method of moments expansion in Legendre polynomials has been employed to obtain the $P^J(E_{\mathrm{c}})$ from the trajectory results.

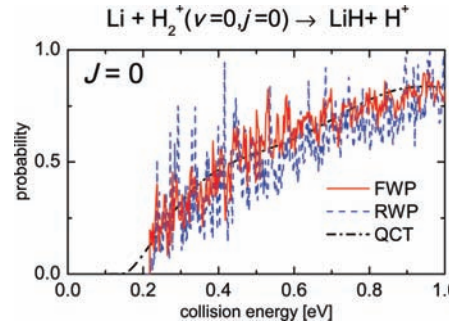

Figure 2. Total reaction probabilities as a function of collision energy at $J = 0$ for the Li + H_2^+ ($v = 0$, $j = 0$) reaction. Solid line: FWP. Dashed line: RWP. Dashed−dot line: QCT.

Excitation functions for the title reaction for $j = 0$ of the H_2^+ molecule have been calculated by running batches of 3×10^5 trajectories at randomly and uniformly sampled collision energies within the range 0.05−1.0 eV. The maximum impact parameter, b_{max}, for the title reaction increases with collision energy. Thus the impact parameter for each trajectory at a given collision energy E_{c} was chosen by randomly sampling between zero and a maximum value of $b_{\mathrm{max}}(E_{\mathrm{c}})$ given by the expression

$$b_{\mathrm{max}}(E_{\mathrm{c}}) = D(1 - E_{\mathrm{D}}/E_{\mathrm{c}})^{1/2} \quad (26)$$

where the parameters D and E_{D} were obtained previously by fitting the values of the maximum impact parameters found by running small batches of trajectories at several selected E_{c} to the functionality of eq 26. Over the range of E_{c} investigated, b_{max} was found to grow with E_{c}. The parameters used ensure that no reaction occurs at a given E_{c} for values of the impact parameter larger than $b_{\mathrm{max}}(E_{\mathrm{c}})$. With this kind of energy dependent sampling of the maximum impact parameter, each trajectory is weighted by $w_i = b_{\mathrm{max}}^2/D^2$. The j-specific excitation functions, $\sigma(E_{\mathrm{c}})$, were subsequently calculated by selecting the set of trajectories with a given j and using the method of moments expansion in Legendre polynomials.

In all cases, trajectories were started at a distance between the incoming atom, Li, and the center-of-mass of the H_2^+ molecule of 20 Å and a time step of 0.05 fs was used for the integration of the equations of motion. Under these conditions total energy was conserved to better than 1 part in 10^4.

The QCT state-specific rate constants were calculated using eq 16 from the corresponding QCT initial j-dependent excitation functions.

III. Results and Discussion

A. Reaction Probabilities. Figure 2 compares the total reaction probabilities as a function of collision energy for $J = 0$, $P^{J=0}(E_{\mathrm{c}})$, calculated for the Li + H_2^+ ($v = 0$, $j = 0$) reaction using the RWP, FWP and QCT methods from threshold up to 1 eV collision energy. The wave packet probabilities show a threshold energy value of ≈0.217 eV, which corresponds to the endothermicity of the reaction on the PES when the zero point energies of reagents and products are considered. After threshold, the wave packet probabilities increase monotonically up to an average value of 0.8 at collision energies around 1 eV. This behavior is typical of endothermic reactions or reactions with an entrance barrier. A large number of very narrow peaks are observed in the RWP and FWP $P^{J=0}(E_{\mathrm{c}})$ over the whole range of collision energies. The amplitude of the structures decreases with increasing collision energy. The presence of

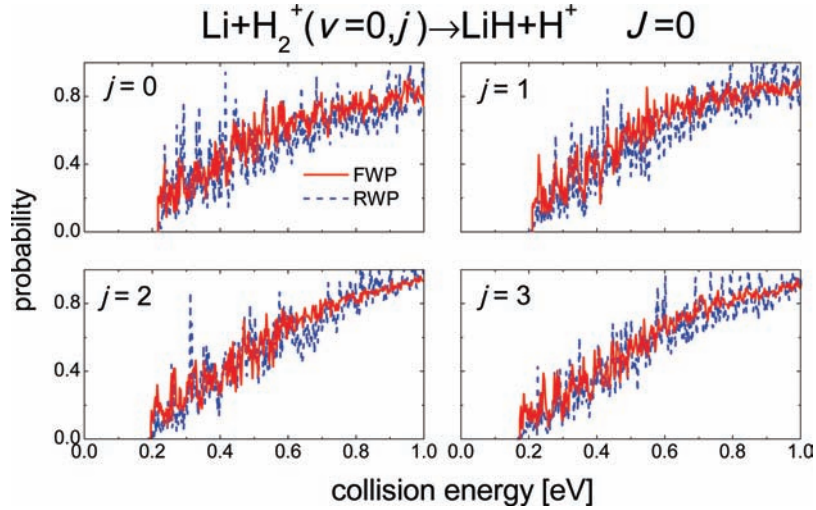

Figure 3. Total reaction probabilities as a function of collision energy at $J = 0$ for the Li + H_2^+ ($v = 0$, $j = 0-3$) reactions. Solid lines: FWP. Dasehd lines: RWP.

resonance structures in the $P^{J=0}(E_c)$ can be expected from the existence of deep wells in the reactant and product valleys that support tiers of quasi-bound states above the dissociation limit of the LiH_2^+ molecular ion and thus, this reaction can be considered as a complex-forming process. The behavior and magnitude of the present total reaction probabilities are very different from those obtained by Gogtas[14] using the same RWP method on the same PES. The discrepancies found can be attributed to a possible lack of convergence in Gogtas' calculations (notice the parameters listed in Table 1 of ref 14 in comparison with those used in the present work shown in Table 2). In principle, the two sets of wave packet calculations presented here (RWP in product Jacobi coordinates and FWP in reactant Jacobi coordinates) should yield essentially the same results if full convergence has been reached. However, the title reaction shows a very dense structure of sharp resonances and, thus, it is difficult to obtain a perfect agreement between the two methods.

The corresponding QCT total reaction probabilities reproduce the overall shape of the wave packet probabilities. However, the QCT calculation predicts an energy threshold somewhat lower as compared with that obtained from the wave packet methods, even though the Gaussian binning procedure is used. This discrepancy found in the QCT $P^{J=0}(E_c)$ can be attributed to the finite width of the GB procedure that allows trajectories with a vibrational energy below the LiH ZPE to contribute to reactivity.

Figure 3 portrays the RWP and FWP total reaction probabilities for $J = 0$ as a function of collision energy for different initial rotational quantum numbers ($j = 0-3$) of the H_2^+ ($v = 0$) reagent. The shape of all reaction probabilities is very similar although the threshold for reaction shifts toward lower energies as the initial rotational quantum state increases, as expected for and endothermic reaction. The agreement between the RWP and FWP calculations is very good.

The centrifugal sudden approximation (CSA) has been applied to calculate wave packet reaction probabilities for total angular momentum $J > 0$. Figure 4 shows the collision energy dependence of the total reaction probability calculated for some selected values of $J > 0$ using the CSA approximation and the FWP method. Very similar results have been obtained using the RWP method (not shown for clarity). In addition, the corresponding QCT results are also displayed for comparison. As J increases, the growth of the centrifugal barrier to reaction give rise to increasing thresholds in the FWP-CSA reaction probabilities. The agreement between FWP-CSA and QCT is generally good. However, for low J values, the threshold energy from the QCT calculations is somehow smaller than that obtained in the FWP-CSA, whereas for large values of J the QCT reaction probabilities clearly underestimate the reactivity in comparison with the FWP-CSA results.

B. Integral Cross Sections and Rate Coefficients. Integral cross sections for the Li+H_2^+($v = 0$, $j = 0$) reaction have been calculated from the FWP-CSA reaction probabilities using the refined J-shifting procedure described in the Method Section in the collision energy range from threshold up to 1 eV, and are shown in Figure 5. Similar results have been obtained using the RWP-CSA calculations (not shown). The corresponding excitation function, $\sigma(E_c)$, obtained by means of the QCT approach using the Gaussian binning procedure is also depicted in Figure 5.

The general shape of both FWP-CSA and QCT $\sigma(E_c)$ is similar, but some interesting discrepancies are found. First, the energy threshold predicted in the QCT calculations is slightly smaller than that derived from the FWP-CSA approach, as it was already noted from the comparison of the total reaction probabilities for $J = 0$. Second, above the threshold energy the QCT excitation function is consistently lower than that obtained by means of the FWP-CSA methodology, indicating that the contribution from resonances and tunnelling is of relative importance in the range of collision energies considered. The monotonic increase of the integral cross section with collision energy found for the title reaction is similar to that found in other endothermic reactions such as $N^+ + H_2$ ($v = 0, j = 0,1$)[23] and H + O_2 ($v = 0 - 2$, $j = 0,1$).[32]

The calculated specific rate coefficients for the Li + H_2^+ ($v = 0$, $j = 0$) reaction derived from Bolztmann averaging of the above FWP-CSA and QCT excitation functions in the temperature range 200−1000 K are displayed in Figure 6. In addition, the rate coefficients obtained by using the SRA from the FWP-CSA calculations are also depicted. The agreement between the FWP-CSA-RefJS and FWP-CSA-SRA rate coefficients is good in the whole temperature range considered and vary from 10^{-15} up to 10^{-11} cm^3 s^{-1}. The corresponding QCT rate coefficients are smaller by a factor of ≈1.5−2. The temperature dependence of the calculated rate coefficients follow a basic Arrhenius behavior. A linear fit of ln($k(T)$) vs $1/T$ yields an activation energy of 0.22 eV for the FWP-CSA-RefJS and FWP-CSA-

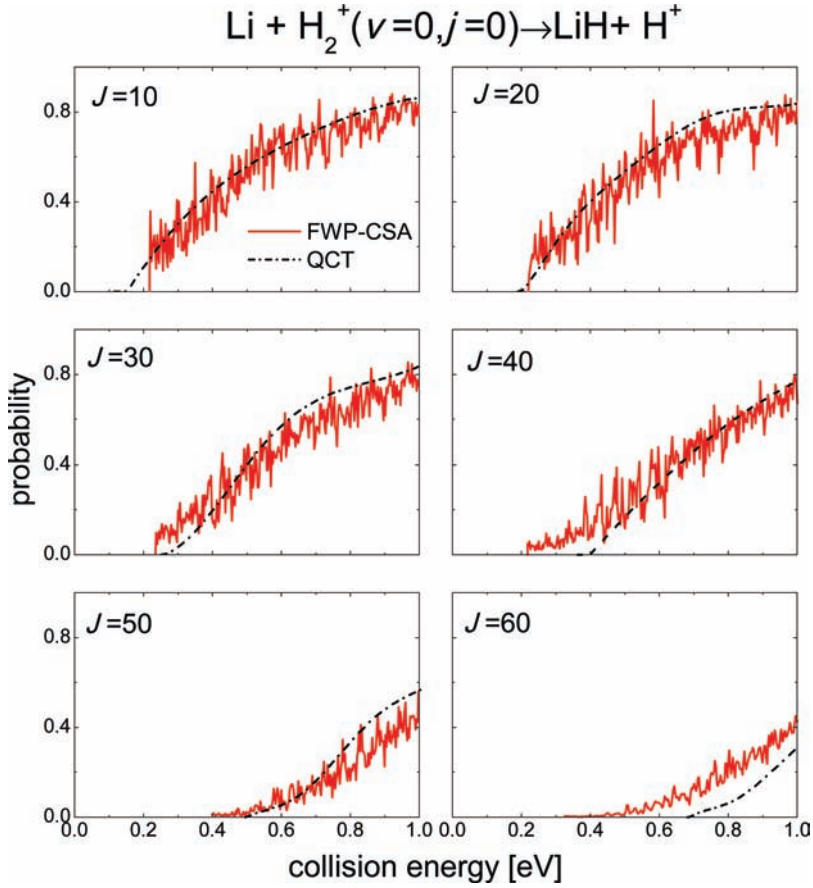

Figure 4. Total reaction probabilities as a function of collision energy for the Li + H_2^+ ($v = 0, j = 0$) reaction for selected values of J calculated using the FWP-CSA and QCT methods. Solid line: FWP-CSA. Dashed-dot line: QCT.

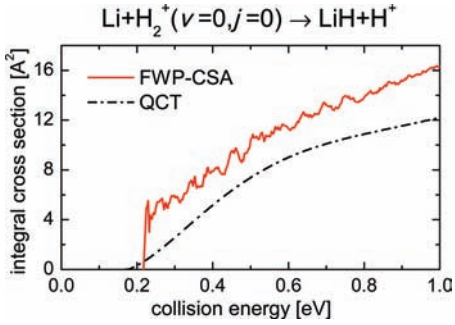

Figure 5. Integral cross-section as a function of collision energy for the Li + H_2^+ ($v = 0, j = 0$) reaction. Solid line: FWP-CSA. Dashed-dot line: QCT.

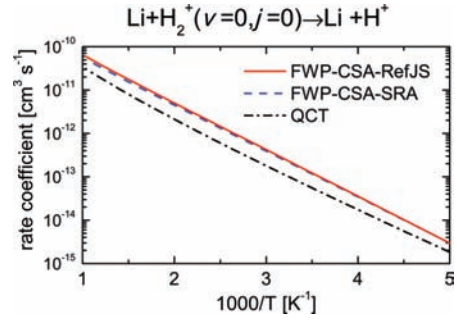

Figure 6. Rate coefficients for the Li + H_2^+ ($v = 0, j = 0$) reaction in the 200−1000 K temperature range. Solid line: FWP-CSA-RefJS. Dashed line: FWP-CSA-SRA. Dashed-dot line: QCT.

SRA rate coefficients, and 0.202 eV for the QCT rate coefficients. The activation energies are in good agreement with the endothermicity of the PES of 0.217 eV. The pre-exponential factors are 4.4×10^{-10} and 6.3×10^{-10} cm^3 s^{-1} for the FWP-CSA-RefJS and FWP-CSA-SRA calculations, respectively, and 3.4×10^{-10} cm^3 s^{-1} for the QCT calculation.

Although the present rate coefficients have been calculated only for the reaction with initial $v = 0$, $j = 0$ state of the H_2^+ reagent, it is expected that the rate coefficients presented in Figure 6 represent a good approximation to the thermal rate coefficients for the title reaction, given the small effect of rotational excitation on reactivity (see Figure 3). The only comparison that can be established between the present rate coefficients and those available in the literature for the title reaction is with the QCT calculations carried out by Pino et al. on the same PES.[15] From their QCT calculations, these authors suggested the following fit for the thermal rate coefficients in the temperature range 600−4000 K: $k/10^{-9}$ cm^3 s^{-1} $= 7.2 \times 10^{-5}(T/K)^{1.18}e^{-1469.8/(T/K)}$. The present wave packet and QCT rate coefficients are in good agreement with the thermal rate coefficients reported by Pino et al. in the 600−1000 K temperature range.

IV. Conclusions

In this work, we have applied the RWP, FWP and QCT methods to study the reactivity of the Li + H_2^+ system on the PES developed by Martinazzo et al.[13] It has been shown that the agreement between RWP, FWP, and QCT total reaction probabilities for $J = 0$ is fairly good. The main discrepancies found between the wave packet and quasiclassical trajectory results are due to the dense resonance structure observed in the wave packet calculations that reflects the influence of the deep

wells in the PES on the dynamics of the reaction. Besides, further discrepancies are observed at collision energies near threshold, where the lack of zero-point energy conservation in the QCT calculation is noticeable. A small effect of reagent rotation on reaction probabilities calculated by the RWP and FWP methods has been observed.

Integral cross sections as a function of collision energy (excitation function) for the title reaction have been calculated using the FWP method within the centrifugal sudden approximation (CSA) to calculate reaction probabilities for total angular momentum $J > 0$ and a refined J-shifting model and by means of QCT calculations. FWP-CSA and QCT excitation functions show the same behavior; that is, they are increasing functions with collision energy, typical of endothermic reactions occurring through a deep well. The calculated FWP-CSA-RefJS, FWP-CSA-SRA, and QCT rate coefficients are in good agreement and show a temperature dependent behavior which is consistent with a simple Arrhenius model.

Acknowledgment. We dedicate this paper to Professor Vincenzo Aquilanti whose long and fruitful scientific carrier has served as an example to several generations of researchers in the field of Reaction Dynamics. N.B. acknowledges a postdoctoral fellowship by Spanish MEC under the program "Estancias de jóvenes doctores y tecnólogos extranjeros en España". This work has received financial support from the Spanish Ministry of Science and Innovation through grant no. CTQ2008-02578/BQU and from the Comunidad de Madrid under the Contrato Programa Comunidad de Madrid-Universidad Complutense de Madrid (Grant No. 910729).

References and Notes

(1) Lepp, S.; Stancil, P. C.; Dalgarno, A. *J. Phys. B: At. Mol. Phys.* **2002**, *35*, R57.
(2) Lepp, S.; Shull, M. *Astrophys. J.* **1984**, *280*, 465.
(3) Palla, F.; Galli, D.; Silk, J. *Astrophys. J.* **1995**, *451*, 44.
(4) Stancil, P. C.; Lepp, S.; Dalgarno, A. *Astrophys. J.* **1996**, *458*, 401.
(5) Stancil, P. C.; Dalgarno, A. *Astrophys. J.* **1997**, *458*, 543.
(6) Galli, D.; Palla, F. *Astron. Astrophys.* **1998**, *335*, 403.
(7) Stancil, P. C.; Lepp, S.; Dalgarno, A. *Astrophys. J.* **1998**, *509*, 1.
(8) Bodo, E.; Gianturco, F. A.; Martinazzo, R. *Phys. Rep.* **2003**, *384*, 85.
(9) Bodo, E.; Gianturco, F. A.; Martinazzo, R.; Forni, A.; Famulari, A.; Raimondi, M. *J. Phys. Chem. A* **2000**, *104*, 11972.
(10) Bodo, E.; Gianturco, F. A.; Martinazzo, R.; Raimondi, M. *Chem. Phys.* **2001**, *271*, 309.
(11) Bodo, E.; Gianturco, F. A.; Martinazzo, R.; Raimondi, M. *J. Phys. Chem. A* **2001**, *105*, 986.
(12) Martinazzo, R.; Bodo, E.; Gianturco, F. A.; Raimondi, M. *Chem. Phys.* **2003**, *287*, 335.
(13) Martinazzo, R.; Tantardini, G. F.; Bodo, E.; Gianturco, F. A. *J. Chem. Phys.* **2003**, *119*, 11241.
(14) Gogtas, F. *J. Chem. Phys.* **2005**, *123*, 244301.
(15) Pino, I.; Martinazzo, R.; Tantardini, G. F. *Phys. Chem. Chem. Phys.* **2008**, *10*, 5545.
(16) Bulut, N.; Castillo, J. F.; Aoiz, F. J.; Bañares, L. *Phys. Chem. Chem. Phys.* **2008**, *10*, 821.
(17) Gray, S. K.; Balint-Kurti, G. G. *J. Chem. Phys.* **1998**, *108*, 950.
(18) Balint-Kurti, G. G.; Gonzalez, A. I.; Goldfield, E. M.; Gray, S. K. *Faraday Discuss.* **1998**, *110*, 169.
(19) Hankel, M.; Balint-Kurti, G. G.; Gray, S. K. *Int. J. Quantum Chem.* **2003**, *92*, 205.
(20) Miller, W. H. *J. Chem. Phys.* **1974**, *61*, 1823.
(21) Miller, W. H.; Schwartz, S. D.; Tromp, J. W. *J. Chem. Phys.* **1983**, *79*, 4889.
(22) Neuhauser, D. *J. Chem. Phys.* **1994**, *100*, 9272.
(23) Russell, C. L.; Manolopoulos, D. E. *J. Chem. Phys.* **1999**, *110*, 177.
(24) Feit, M. D.; Fleck, J. A. *J. Chem. Phys.* **1983**, *78*, 301.
(25) Pack, R. T. *J. Chem. Phys.* **1974**, *60*, 633.
(26) Bowman, J. M. *J. Phys. Chem.* **1991**, *95*, 4960.
(27) Mielke, S. L.; Lynch, C. C.; Truhlar, D. C.; Schwenke, D. W. *J. Phys. Chem.* **1994**, *98*, 8000.
(28) Zhang, D. H.; Zhang, J. Z. H. *J. Chem. Phys.* **1999**, *110*, 7622.
(29) Aoiz, F. J.; Banares, L.; Herrero, V. J. *J. Chem. Soc. Faraday Trans.* **1998**, *94*, 2483.
(30) Bonnet, L.; Rayez, J. C. *Chem. Phys. Lett.* **1997**, *277*, 183.
(31) Bañares, L.; Aoiz, F. J.; Honvault, P.; Bussery-Honvault, B.; Launay, J.-M. *J. Chem. Phys.* **2003**, *118*, 565.
(32) Lin, S. Y.; Sun, Z.; Guo, H.; Zhang, D. H.; Honvault, P.; Xie, D.; Lee, S.-Y. *J. Phys. Chem. A* **2008**, *112*, 602.

JP904429E